International Communication in Computational Mechanics

Journal homepage:
https://karyailham.com.my/index.php/iccm
ISSN: 3093-7205

Analysis of Heat and Mass Transfer in Nonlinear Magnetohydrodynamic Flow Considering Dissipation Effects Induced by a Stretching Surface with Variable Temperature

Anne Susan Georgena. S[1], Rohana Abdul Hamid[2,3,*],Nor Ashikin Abu Bakar[2]

[1] Department of Mathematics, Sri Ramakrishna Institute of Technology, Coimbatore, India
[2] Institute of Engineering Mathematics, Universiti Malaysia Perlis, Pauh Putra Campus, 02600 Arau, Perlis, Malaysia
[3] Centre of Excellence for Social Innovation and Sustainability (CoESIS), Universiti Malaysia Perlis, Pauh Putra Campus, 02600 Arau, Perlis, Malaysia

ARTICLE INFO

Article history:
Received 4 November 2024
Received in revised form 17 November 2024
Accepted 2 December 2024
Available online 15 March 2025

Keywords:
MHD; viscous dissipation; stretching surface; heat and mass transfer; porous medium

ABSTRACT

This paper investigates heat and mass transfer phenomena in nonlinear magnetohydrodynamic, steady, laminar, boundary layer flow of a viscous, incompressible electrically conducting fluid over a stretching surface subject to suction with variable temperature in the presence of a uniform transverse magnetic field and temperature gradient dependent heat sink. The analysis considers the impact of viscous and Ohmic dissipation, which significantly influence thermal and concentration distributions. Similarity transformations are used to derive and convert governing partial differential equations into a collection of nonlinear ordinary differential equations. The precise solution of the momentum equation has been derived. By incorporating relevant similarity variables, the energy equation and the species concentration equation are converted into nonlinear ordinary differential equations, which are subsequently resolved using confluent hypergeometric functions. Coding for this problem was executed in Fortran 77 language and output exported to Axum for graphs. The impact of several physical parameters on the profiles of temperature, concentration, and velocity is investigated, including the magnetic field, Prandtl number, Eckert number, and Schmidt number. Graphical and tabular representations illustrate the role of dissipation and surface stretching on the characteristics of the transmission of thermal and mass transfer, with key findings highlighting the practical applications in industrial processes and materials engineering. Additionally, the skin friction at the wall is measured and graphically shown.

1. Introduction

Flow through a stretching surface using magnetohydrodynamics (MHD) has garnered substantial focus due to its broad applications in fields like metallurgy, polymer extrusion, and aerospace engineering. The interaction of magnetic fields with electrically conducting fluids enhances heat and

* *Corresponding author.*
E-mail address: rohanahamid@unimap.edu.my

https://doi.org/10.37934/iccm.1.1.113

mass transfer, making it crucial for industrial processes. To be more precise, a lot of metallurgical procedures entail cooling continuous strips by dragging them over stagnant fluid. During the drawing process, the strips are sometimes stretched. The fundamental concept of boundary-layer flow over a stretching sheet was introduced by Sakiadis [1]. Since then, various researchers have extended this model to include MHD effects, heat transfer, and viscous dissipation.

In today's era of technological progress, industries are increasingly adopting advanced technologies for extraction and manufacturing. In these processes, extruded materials are drawn from the dye and stretched into filaments, solidifying into the desired shape through precisely controlled cooling systems. Therefore, many authors including Takhar *et al*., [2], Devi and Thiyagarajan [3], Gopal *et al*., [4] and Alzahrani *et al.*, [5] have examined boundary layer flow issues brought on by a stretching sheet.

Following the pioneering research of Sakiadis [1], Crane [6] extended the analysis by considering linear stretching, setting the stage for magnetohydrodynamic (MHD) applications. Subsequent research focused on incorporating the effects of magnetic fields, with Andersson et al., [7] exploring MHD flow with variable surface temperatures and different fluid behaviors. These studies established the importance of magnetic fields in controlling the transmission of thermal and mass processes.

Vajravelu and Nayfeh [8] focused on convective heat transfer in electrically conducting fluids under a constant transverse magnetic field. This study highlighted the impact of magnetic fields on enhancing thermal stability and controlling convective flows in MHD applications. Chiam [9] examined the power-law velocity pattern of boundary layer flow across a surface that is stretching. Through incorporating a transverse magnetic field, Chiam demonstrated that magnetic fields could effectively control the boundary layer thickness, contributing to optimized heat transfer in industrial processes. Building upon Chiam's work, recent studies such as Ali *et al*., [10] have further explored electrically conducting mixed convective nanofluid flow past a nonlinearly slender Riga plate, considering effects like viscous dissipation and activation energy. Their findings emphasize the continued relevance of magnetic fields in manipulating boundary layer characteristics and enhancing heat and mass transfer. Similarly, Waqas *et al*., [11] conducted a numerical analysis of MHD tangent hyperbolic nanofluid flow over a stretching surface subject to heat source or sink effects. This research extends the understanding of non-Newtonian fluid behavior in MHD flows and reinforces the importance of magnetic fields and thermal effects in industrial heat transfer processes.

Advancements with temperature distributions were made by Grubka and Bobba [12]. They investigated the transfer of heat over a linearly stretching surface, incorporating power-law temperature distributions. This study laid the groundwork for understanding non-uniform heating effects and their influence on boundary layer behavior. Chen and Char [13] extended the analysis by considering both prescribed wall temperatures and heat flux conditions, including suction effects. Their work involved solving the energy equation using the Kummer function, derived from the linear confluent hypergeometric differential equation, a significant mathematical development that offered exact solutions for complex thermal systems.

Ohmic and Joule dissipation became focal points in the early 2000s. Swain *et al*., [14] investigated the impact of viscous dissipation and Joule heating on magnetohydrodynamic (MHD) flow and heat transfer past a stretching sheet embedded in a porous medium. The findings highlight that these effects significantly enhance heat transfer rates, particularly in engineering applications involving electrically conductive fluids and porous structures. Viscous dissipation was found to significantly affect boundary layer stability and temperature distribution, leading to improved models for industrial cooling systems. Abel *et al.,* [15] analyzed viscoelastic MHD flow and heat transfer over a stretching sheet, highlighting the role of viscous and ohmic dissipations.

Anjalidevi and Kayalvizhi [16] explored nonlinear hydromagnetic flow with radiation and a heat source over a stretching surface, focusing on cases with prescribed heat and mass flux embedded in a porous medium. Their study examines how radiative heat transfer and magnetic fields interact with flow dynamics in porous media. Key findings emphasize the significant role of thermal radiation in altering boundary layer behavior, affecting temperature distribution and velocity profiles.

However, it is important to note that most studies neglect Ohmic dissipation (Joule heating), even though it is critical in many industrial and practical applications involving MHD flows. Moreover, while many authors rely on numerical techniques to solve the transformed equations, very few studies provide exact solutions for boundary layer flows with dissipation effects. This study addresses these gaps by presenting an exact analytical solution for MHD flow over a stretching sheet, explicitly incorporating viscous and Ohmic dissipation effects. This approach provides a deeper theoretical understanding of the interactions between magnetic fields, heat transfer, and mass transfer, which are often simplified in numerical studies. Furthermore, the inclusion of Ohmic dissipation enhances the applicability of the results to real-world industrial scenarios such as metallurgical cooling systems, material extrusion, and MHD flow control.

This overview highlights significant progress and evolving themes in the MHD flow research with thermal and mass transmission, reflecting the growing complexity and relevance of these models in modern engineering applications. By assuming suitable transformations, the exact solution of the momentum equation is obtained. The energy equation and the species concentration equation are transformed using similarity variables into nonlinear ODE's and are solved using confluent hypergeometric functions by utilizing suitable transformations. Fixing different parameters yields the numerical values of the solutions for the physical parameters and are plotted graphically.

2. Mathematical Formulation

This research investigates the two-dimensional steady flow of an incompressible, viscous, and electrically conducting fluid within a hydromagnetic boundary layer. The flow occurs over a stretching sheet influenced by a uniform transverse magnetic field, heat sink, and dissipation effects. The sheet experiences variable temperature and steady suction, with the surrounding medium being porous.

The surface experiences a non-uniform magnetic field $\underline{B}(x) = B(x)\hat{j}$ in the transverse direction. The velocity at a specific position upon the sheet or wall is considered as proportional to its distance from the origin, and it is assumed that the components of velocity are (u,v) and that the wall sheet emerges from a thin slit at the origin (0,0). The approximations for the boundary layer remain valid. The subsequent boundary layer equations now govern the problem when the induced magnetic field, which is permitted at lower magnetic Reynolds numbers, is neglected.

2.1 Momentum Distribution

Adopting the above assumptions and following the lines of Vafai and Tien's model [17], the boundary layer equations of steady MHD flow are given by the following equations.

$$\frac{\partial u}{\partial x}+\frac{\partial v}{\partial y}=0 \tag{1}$$

$$u\frac{\partial u}{\partial x}+v\frac{\partial v}{\partial y}=\nu\frac{\partial^2 u}{\partial y^2}-\frac{\nu}{K_p}u-\frac{\sigma {B_0}^2}{\rho}u \tag{2}$$

together with the relevant boundary conditions

at y= 0, u = U(x) = U_0 x = a x , v = -v_0 (a>0) (3)
as y→ ∞, u→0,

In deriving the above equations, the induced magnetic field is assumed negligible when it is much smaller than the applied magnetic field. Additionally, as $div\vec{E}=0$ and $curl\vec{E}=0$, $\vec{E}=0$ i.e., the external electric field is zero and the electric field resulting from charge polarization is considered insignificant.

Given ψ is the stream function in Eq. (4), which is defined by the following relationship and is used to explain the solution to Eq. (1):

$$u=\frac{\partial\psi}{\partial y}, \qquad v=-\frac{\partial\psi}{\partial x} \tag{4}$$

In accordance with Banks [18] and Afzal [19], the following similarity variables are presented such that in Eq. (5);

$$\psi(x,y)=x\sqrt{a\nu}\,F(\eta),\ \eta=y\sqrt{\frac{a}{\nu}} \tag{5}$$

where the similarity space variable is given by η and $F(\eta)$ is the dimensionless stream function. Consequently, we have

$$u=a\,x\,F'(\eta),\ \ v=-\sqrt{\nu a}\,F(\eta) \tag{6}$$

Equation of continuity given by (1) is obviously satisfied by (6). Hence, when (6) is substituted in Eq. (2), we get

$$F'''+FF''-F'^2-(M^2+1/R)F'=0 \tag{7}$$

where ' refer the permeability parameter is $R=\frac{K_p a}{\nu}$ and the magnetic interaction parameter is $M^2=\frac{\sigma B_0^{\,2}}{\rho a}$.

Eq. (5) is utilized to transform the boundary conditions of Eq. (3) into

at $\eta=0,\ F(0)=S,\ F'(0)=1$ (8)
as $\eta\to\infty,\ \ F(\infty)=0$

where $S=\frac{v_0}{a\nu}$ ($v_0>0$) is the suction parameter. According to Chakrabarti and Gupta [20], Eq. (7) admits a solution of the following form:

$$F(\eta) = A + Be^{-E\eta} \tag{9}$$

where, $A = \dfrac{E^2 - (M^2 + 1/R)}{E}$, $B = -1/E$, (10)

$$E = \frac{S + \sqrt{S^2 + 4(M^2 + 1/R + 1)}}{2} \tag{11}$$

Hence the exact solution is,

$$F(\eta) = \frac{1}{E}\left[(E^2 - (M^2 + 1/R)) - e^{-E\eta} \right] \tag{12}$$

$$F'(\eta) = e^{-E\eta} \tag{13}$$

2.2 Temperature Distribution

The boundary layer equation for energy is given by,

$$\rho C_p \left(u\frac{\partial T}{\partial x} + v\frac{\partial T}{\partial y} \right) = k\frac{\partial^2 T}{\partial y^2} + \mu\left(\frac{\partial u}{\partial y}\right)^2 + \sigma B_0^2\, u^2 - Q'\frac{\partial T}{\partial y} \tag{14}$$

Appropriate boundary conditions are given by,

at y=0, $T = T_w(x) = T_\infty + T_0 x^2$ (15)
as $y \to \infty, T \to T_\infty$

To solve the Eq. (14), the following variables are introduced,

$$\theta(\eta) = \frac{T - T_\infty}{T_w - T_\infty}, \quad \eta = y\sqrt{a/\nu} \tag{16}$$

Using Eq. (16) in Eq. (14), it is obtained as

$$\theta''(\eta) + \Pr(1+Q)F(\eta)\theta'(\eta) - 2\Pr F'(\eta)\theta(\eta) = -Ec\Pr\left[F''(\eta)^2 + M^2 F'(\eta)^2 \right] \tag{17}$$

where the Prandtl number and Eckert number are given by $\Pr = \dfrac{\mu C_p}{k}$ and $Ec = \dfrac{U_0^2}{C_p T_0}$ respectively.

The appropriate conditions for the boundary are

at $\eta = 0$, $\eta = 0, \theta(\eta) = 1$ (18)
as $\eta \to \infty$, $\theta(\eta) \to 0$

In Eq. (17), a new variable ξ is added to obtain the solution and it is given by,

$$\xi^{-1} = \frac{-E^2 e^{E\eta}}{\Pr(1+Q)} \tag{19}$$

i.e., $$\xi = \frac{-\Pr(1+Q)}{E^2} e^{-E\eta} \tag{20}$$

Using Eq. (20), the partial differential Eq. (17) is transformed to the following ordinary differential equation

$$\xi \frac{d^2\theta}{d\xi^2} + [\gamma - \xi]\frac{d\theta}{d\xi} + S_1\theta = \left[\frac{-EcE^2}{\Pr(1+Q)^2}\left(E^2 + M^2\right)\right]\xi \tag{21}$$

where $$\gamma = 1 - \frac{\Pr(1+Q)}{E^2}\left[E^2 - (R^{-1} + M^2)\right],\ S_1 = \frac{2}{1+Q}$$

The boundary conditions given by Eq. (18) become as

$$\text{at } \xi = \frac{-\Pr(1+Q)}{E^2},\ \theta(\xi) = 1 \tag{22}$$
$$\text{at } \xi = 0,\ \theta(\xi) = 0$$

Eq. (21) is a nonhomogeneous Confluent hypergeometric equation. Hence, solution of Eq. (21) is thus expressed as,

$$\theta(\xi) = \left[\frac{1 - K_1^2 A\left(\sum_{n=0}^{\infty}\frac{\Gamma(2+n-S_1)\Gamma(2+\gamma)\Gamma(2)}{\Gamma(2-S_1)\Gamma(3+n)\Gamma(2+\nu+n)}(-K_1)^n\right)}{1F1\ (-S_1-\nu+1, 2-\nu, -K_1)\ (-K_1)^{1-\nu}}\xi^{(1-\nu)}1F1\ (-S_1-\nu+1, 2-\nu, \xi)\right] + \left[\xi^2 A\left(\sum_{n=0}^{\infty}\frac{\Gamma(2-S_1+n)\Gamma(2)\Gamma(2+\nu-1)}{\Gamma(2-S_1)\Gamma(3+n)\Gamma(2+\nu+n)}\xi^n\right)\right] \tag{23}$$

where $K_1 = \frac{\Pr(1+Q)}{E^2}$, $A = \frac{-EcE^2}{\Pr(1+Q)^2}[E^2 + M^2]$

The following is an expression for the function θ with respect to variable η.

$$\theta(\eta) = \left(1 - K_1^2 A\left(\sum_{n=0}^{\infty}\frac{\Gamma\left(2+n-s_1\Gamma\left(1+\nu\right)\Gamma\left(2\right)\right)}{\Gamma\left(2-s_1\right)\Gamma\left(3+n\right)\Gamma\left(2+\nu+n\right)}\left(-K_1\right)^n\right)\right) \cdot \left(\frac{\left(-K_1 e^{-E\eta}\right)^{1-\nu} 1F1\left(-S_1-\nu+1, 2-\nu, -K_1 e^{-E\eta}\right)}{1F1\left(-S_1-\nu+1, 2-\nu, -K_1\right)\left(-K_1\right)^{1-\nu}}\right) + \left(K_1^2 e^{-2E\eta} A\sum_{n=0}^{\infty}\frac{\Gamma\left(2+n-S_1\right)\Gamma\left(1+\nu\right)\Gamma\left(2\right)}{\Gamma\left(2-S_1\right)\Gamma\left(3+n\right)\Gamma\left(2+\nu+n\right)}\left(-K_1 e^{-E\eta}\right)^n\right) \tag{24}$$

2.3 Concentration Distribution

The species concentration equation is provided by,

$$u\frac{\partial C}{\partial x}+v\frac{\partial C}{\partial y}=D\frac{\partial^2 C}{\partial y^2} \tag{25}$$

where C is the species concentration of the fluid, C_∞ is the species concentration of the fluid far from the wall and D is the diffusivity coefficient. The boundary conditions are

$$\text{at y=0, } C=C_w(x)=C_\infty+C_0 x \tag{26}$$
$$\text{as } y\to\infty, C\to C_\infty$$

where C_0 is a dimensional constant.

$$\text{Define} \qquad h=\frac{C-C_\infty}{C_w-C_\infty} \tag{27}$$

Using Eq. (27) in equation Eq. (25), we obtain

$$h''(\eta)-Sch(\eta)F'(\eta)+ScF(\eta)h'(\eta)=0 \tag{28}$$

where Schmidt number is given by $Sc=\frac{\upsilon}{D}$. The following are the boundary conditions for Eq. (28),

$$\text{at } \eta=0, h(\eta)=1 \tag{29}$$
$$\text{as } \eta\to\infty, h(\eta)\to 0$$

A new variable ζ is included in order to get the answer to Eq. (28), which is given by

$$\zeta^{-1}=\frac{-E^2e^{E\eta}}{Sc}\ , \qquad \zeta=\frac{-Sc}{E^2}e^{-E\eta} \tag{30}$$

Using Eq. (30), the Eq. (28) is transformed into the following ordinary differential equation and it is given by

$$\zeta\frac{d^2h}{d\zeta^2}+[\gamma_1-\zeta]\frac{dh}{d\zeta}+S_2h=0 \tag{31}$$

$$\text{where } S_2=1\ ;\ \gamma_1=\frac{Sc}{E^2}\left[E^2-(M^2+\frac{1}{R})\right] \tag{32}$$

Eq. (31) is a homogeneous Confluent hypergeometric equation. The following boundary conditions are utilized in order to solve Eq. (31).

at $\zeta = 0, h(\zeta) = 0$ (33)
as $\zeta = \frac{-Sc}{E^2}, h(\zeta) = 1$

we have

$$h(\zeta) = \frac{\zeta^{1-\gamma_1} 1F1 \quad (-S_2 - \gamma_1 + 1, 2 - \gamma_1, \zeta)}{\left(\frac{-Sc}{E^2}\right)^{1-\gamma_1} 1F1\left(-S_2 - \gamma_1 + 1, 2 - \gamma_1, -\frac{Sc}{E^2}\right)} \tag{34}$$

2.4 Wall Shear Stress

The dimensionless shear stress at the wall is calculated. The wall shear stress is given by

$$\tau = \mu \left(\frac{\partial u}{\partial y}\right)_{y=0} \tag{35}$$

and the coefficient of local shear stress is given by,

$$\tau^* = F''(0) = -E \tag{36}$$

3. Results

Numerical values were obtained by assigning specific typical values to the physical parameters, and the results were visually represented to clearly illustrate their physical effects. The coding for this problem was implemented in Fortran 77, and the output was exported to Axum for graphical visualization.

Figure 1 illustrates how the magnetic field affects the dimensionless transverse velocity F(η). It is evident that the transverse velocity is slowed down by the magnetic field. It is also noteworthy that the magnetic field's effect becomes consistent as we get farther away from the wall. However, the effect of magnetic field and suction have differing effects on transverse velocity. Porosity has the effect of increasing transverse velocity. As illustrated in Figure 2, the effect of porosity remains constant for any value of S as we move away from the wall.

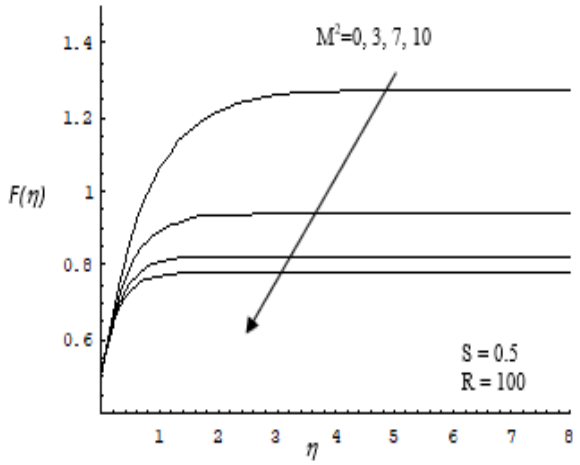

Fig. 1. Effect of magnetic field on dimensionless transverse velocity

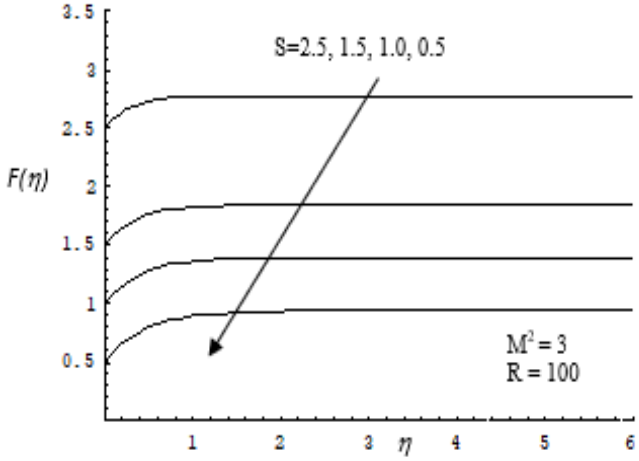

Fig. 2. Dimensionless transverse velocity profiles for various values of *S*

The impact of the magnetic field on the longitudinal dimensionless velocity profiles is depicted in Figure 3. Magnetic fields generally have the dual effects of decreasing the thickness of the boundary layer and slowing down the dimensionless longitudinal velocity. Figure 4 shows how porosity affects non dimensional longitudinal velocity. All profiles converge asymptotically to the horizontal axis, and it is found that a rise in S is accompanied by a constant drop in longitudinal velocity. In every instance, the nondimensional longitudinal velocity is found to be at its highest at the wall. It is also observed that porosity has the effect of decreasing the thickness of the boundary layer.

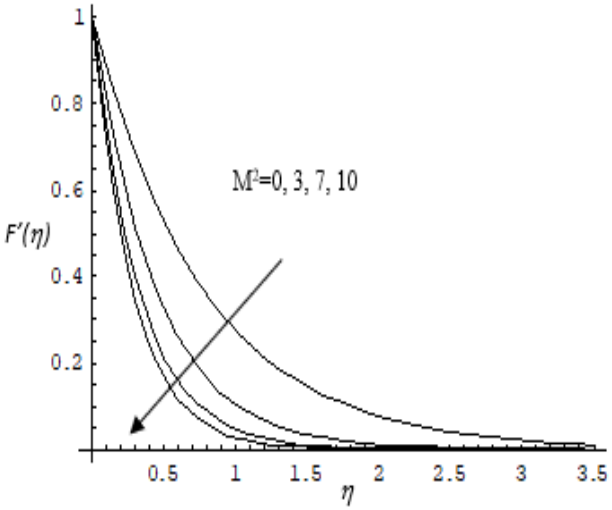

Fig. 3. Dimensionless longitudinal velocity profiles for different values of M^2

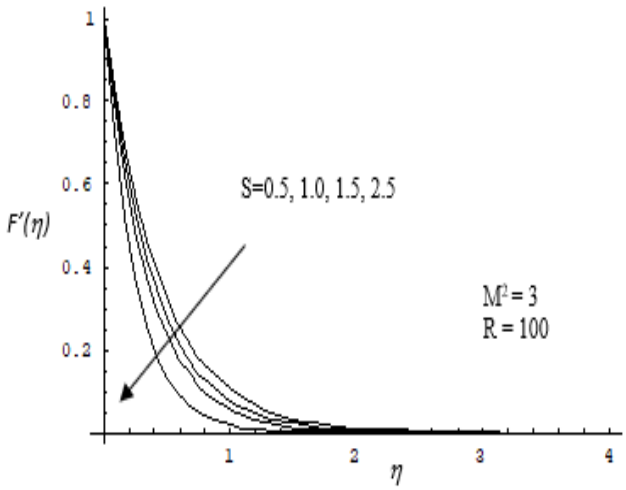

Fig. 4. Dimensionless longitudinal velocity profiles for various values of S

The nondimensional temperature profiles for various M^2 values are shown in Figure 5. When there is suction present, the magnetic field causes the temperature field to rise. Meanwhile in Figure 6 shows the variation in dimensionless temperature caused by the change in suction parameter S. The temperature decreases as the suction parameter S rises.

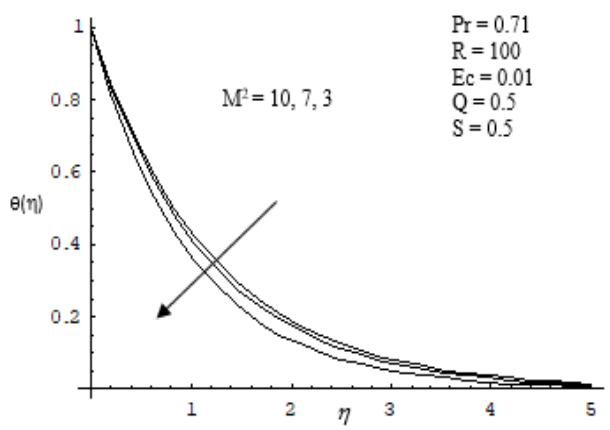

Fig. 5. Influence of M^2 over temperature distribution

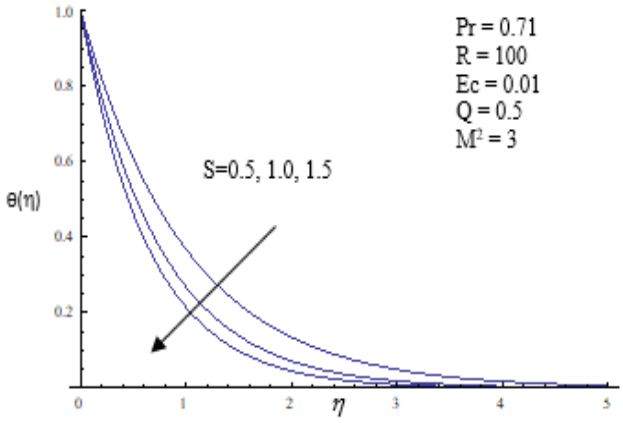

Fig. 6. Effect of S over temperature distribution

Figure 7 shows non-dimensional temperature trends for different values of the parameter Q. It is observed that when Q rises, the temperature field falls and that the higher temperatures are only visible close to the wall. The dimensionless temperature curves for different Eckert number values are shown in detail in Figure 8. The temperature rises in tandem with Ec.

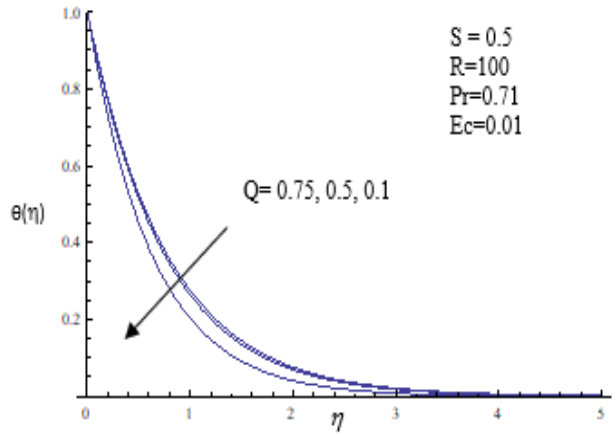

Fig. 7. Influence of Q over temperature distribution

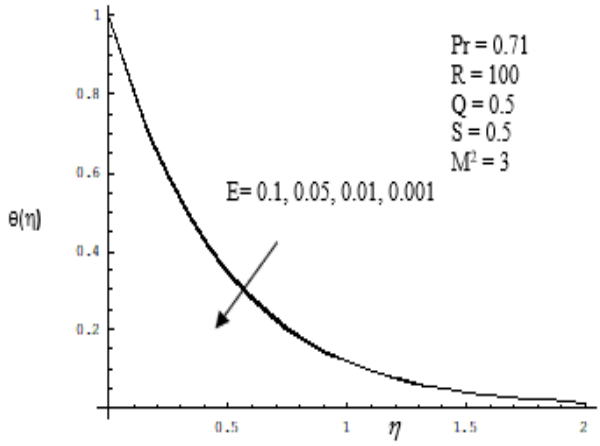

Fig. 8. Influence of Ec over temperature distribution

The impact of the magnetic field on the distribution of concentration is seen in Figure 9. The concentration rises in tandem with M^2. Near the wall, concentration reaches its peak. The non-dimensional distribution of concentration for a range of suction parameter values is shown in Figure 10. The species concentration falls as the suction parameter rises. In this case, too, the species concentration rises only at the stretched sheet.

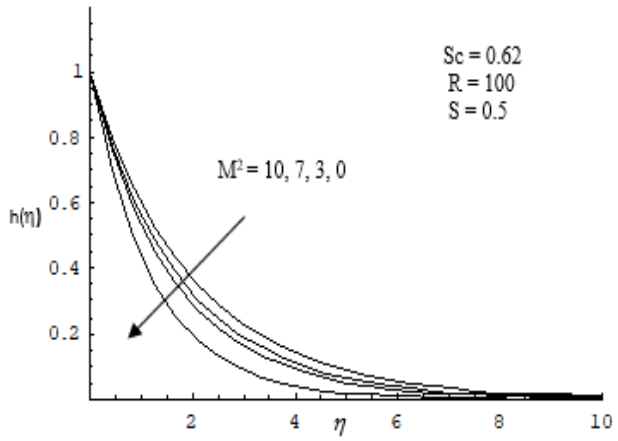

Fig. 9. Influence of M^2 on concentration distribution

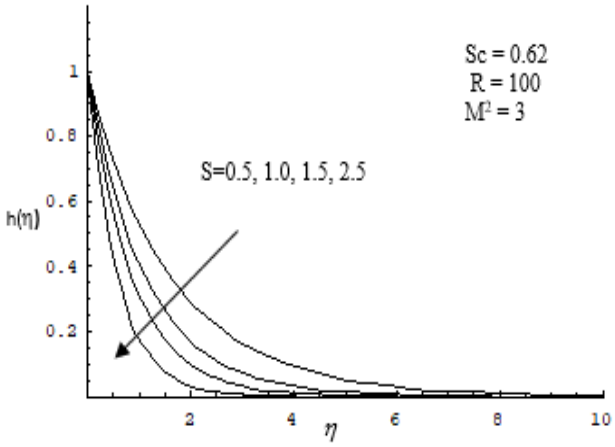

Fig. 10. Dimensionless concentration distribution for different values of S

For a range of magnetic interaction parameter values, Figure 11 shows the wall shear stress against the permeability parameter. Skin friction is suppressed by the magnetic field and stays constant when it is not in contact with the wall. Lastly, Figure 12 is used to investigate the variation in the skin friction coefficient for various porosity parameter values. The skin friction coefficient is reduced because of suction and porosity.

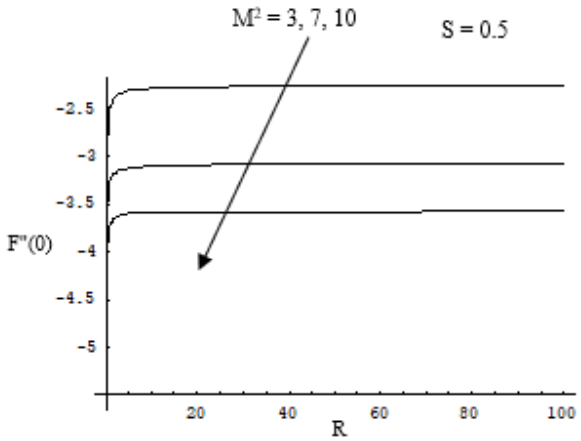

Fig. 11. Skin friction coefficient for various values of M^2

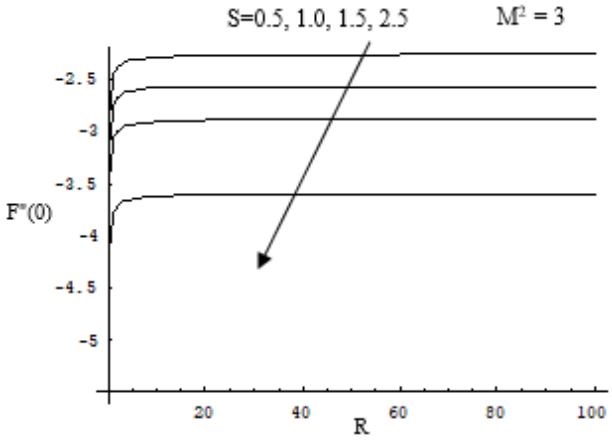

Fig. 12. Skin friction coefficient for various values of S

4. Conclusions

This study has explored the temperature, concentration, and velocity distributions in a nonlinear MHD flow with dissipation effects over a stretching surface under the effect of various parameters, such as the suction parameter (S), magnetic interaction parameter (M^2), permeability parameter (R), heat sink parameter (Q), Prandtl number (Pr), Eckert number (Ec), and Schmidt number (Sc). Key findings include:

i. Velocity Distributions:
   a) Both longitudinal and transverse velocities are significantly affected by the magnetic field (M^2), suction (S), and permeability (R).
   b) Magnetic fields slow down the transverse and longitudinal velocities, reducing boundary layer thickness.

c) Suction decreases longitudinal velocity, while porosity increases transverse velocity, especially near the surface.

ii. Temperature Distributions:
   a) Temperature increases with the magnetic interaction parameter (M^2) and the Eckert number (Ec) but decreases with higher suction (S), Prandtl number (Pr), and heat sink parameter (Q).
   b) Suction enhances heat transfer by reducing the temperature near the surface, while higher values of Q show significant temperature reduction.

iii. Concentration Distributions:
   a) The concentration profile is influenced similarly by parameters affecting the temperature distribution. The magnetic field (M^2) increases concentration, while suction (S) and the Schmidt number (Sc) decrease it.
   b) Maximum concentration occurs near the wall, with notable suppression due to increased suction and Schmidt number.

iv. Skin Friction:
   a) Magnetic fields and suction parameters reduce skin friction, which stabilizes away from the surface.
   b) Porosity also reduces skin friction, indicating its potential role in optimizing boundary layer flow.

Overall, the results highlight the critical roles of magnetic fields, suction, and permeability in controlling heat and mass transfer characteristics in MHD flows. These insights can be applied to optimize industrial processes, such as material extrusion and thermal management systems, where magnetic fields and fluid dynamics play essential roles. The graphical illustrations further provide a clear understanding of these physical phenomena, offering valuable guidance for practical applications.

Acknowledgement
This research was not funded by any grant.

References

[1] Sakiadis, Byron C. "Boundary-layer behavior on continuous solid surfaces: I. boundary-layer equations for two-dimensional and axisymmetric flow." *AIChE Journal* 7, no. 1 (1961): 26–28. https://doi.org/10.1002/aic.690070108.
[2] Takhar, Harmindar S., Ali J. Chamkha, and Girishwar Nath. "Flow and mass transfer on a stretching sheet with a magnetic field and chemically reactive species." *International Journal of Engineering Science* 38, no. 12 (2000): 1303-1314. https://doi.org/10.1016/S0020-7225(99)00079-8
[3] Anjali Devi, S. P., and M. Thiyagarajan. "Steady nonlinear hydromagnetic flow and heat transfer over a stretching surface of variable temperature." *Heat and Mass Transfer* 42 (2006): 671-677. https://doi.org/10.1007/s00231-005-0640-y
[4] Gopal, D., S. Jagadha, P. Sreehari, N. Kishan, and D. Mahendar. "A numerical study of viscous dissipation with first-order chemical reaction and ohmic effects on MHD nanofluid flow through an exponential stretching sheet." *Materials Today: Proceedings* 59, (2022): 1028-1033. https://doi.org/10.1016/j.matpr.2022.02.368
[5] Alzahrani, Jawaher, Hanumesh Vaidya, K. V. Prasad, C. Rajashekhar, D. L. Mahendra, and Iskander Tlili. "Micro-polar fluid flow over a unique form of vertical stretching sheet: Special emphasis to temperature-dependent properties." *Case Studies in Thermal Engineering* 34, (2022): 102037. https://doi.org/10.1016/j.csite.2022.102037
[6] Crane, L. J. "Flow past a stretching plate." *ZAMP* 21, no. 6 (1970): 645-647.https://doi.org/10.1007/BF01587695
[7] Andersson, H. I., K. H. Bech, and B. S. Dandapat. "Magnetohydrodynamic flow of a power-law fluid over a stretching sheet." *International Journal of Non-Linear Mechanics* 27, no. 6 (1992): 929-936. https://doi.org/10.1016/0020-7462(92)90045-9

[8] Vajravelu, K., and J. Nayfeh. "Convective heat transfer at a stretching sheet." *Acta Mechanica* 96, no. 1 (1993): 47-54. https://doi.org/10.1007/BF01340699

[9] Chiam, T. C. "Hydromagnetic flow over a surface stretching with a power-law velocity." *International Journal of Engineering Science* 33, no. 3 (1995): 429-435. https://doi.org/10.1016/0020-7225(94)00066-S

[10] Ali, Bilal, Sidra Jubair, Zafar Mahmood, and Md Irfanul Haque Siddiqui. "Electrically conducting mixed convective nanofluid flow past a nonlinearly slender Riga plate subjected to viscous dissipation and activation energy." *Modern Physics Letters B* 38, no. 33 (2024): 2450336. https://doi.org/10.1142/S0217984924503366

[11] Waqas, Muhammad, Mariam Redn Almutiri, Budur Yagoob, Hijaz Ahmad, and Muhammad Bilal. "Numerical analysis of MHD tangent hyperbolic nanofluid flow over a stretching surface subject to heat source/sink." *Pramana* 98, no. 1 (2024): 27. https://doi.org/10.1007/s12043-023-02702-1

[12] Grubka, L. J., and K. M. Bobba. "Heat transfer characteristics of a continuous stretching surface with variable temperature." *Journal of Heat Transfer* 107, no. 1 (1985): 248-250. https://doi.org/10.1115/1.3247387

[13] C. K. Chen, and M. I. Char. "Heat transfer of a continuous, stretching surface with suction or blowing." *Journal of Mathematical Analysis and Applications* 135, no. 2 (1988): 568-580. https://doi.org/10.1016/0022-247X(88)90172-2

[14] Swain, B. K., B. C. Parida, S. Kar, and N. Senapati. "Viscous dissipation and joule heating effect on MHD flow and heat transfer past a stretching sheet embedded in a porous medium." *Heliyon* 6, no. 10 (2020). https://doi.org/10.1016/j.heliyon.2020.e05338

[15] Abel, M. Subhas, Emmanuel Sanjayanand, and Mahantesh M. Nandeppanavar. "Viscoelastic MHD flow and heat transfer over a stretching sheet with viscous and ohmic dissipations." *Communications in Nonlinear Science and Numerical Simulation* 13, no. 9 (2008): 1808-1821.

[16] Anjalidevi, S. P., and M. Kayalvizhi. "Nonlinear hydromagnetic flow with radiation and heat source over a stretching surface with prescribed heat and mass flux embedded in a porous medium." *Journal of Applied Fluid Mechanics* 6, no. 2 (2013): 157-165. https://doi.org/10.36884/jafm.6.02.19510

[17] Vafai, Kambiz, and Chang L. Tien. "Boundary and inertia effects on flow and heat transfer in porous media." *International Journal of Heat and Mass Transfer* 24, no. 2 (1981): 195-203. https://doi.org/10.1016/0017-9310(81)90027-2

[18] Banks, W. H. H. "Similarity solutions of the boundary-layer equations for a stretching wall." *Journal de Mécanique théorique et appliquée* 2, no. 3 (1983): 375-392.

[19] Afzal, Noor. "Heat transfer from a stretching surface." *International Journal of Heat and Mass Transfer* 36, no. 4 (1993): 1128-1131.

[20] Chakrabarti, A., and A. S. Gupta. "Hydromagnetic flow and heat transfer over a stretching sheet." *Quarterly of Applied Mathematics* 37, no. 1 (1979): 73-78.